

## **Sequences distribution of poly(ethylene terephthalate-isophthalate) copolymers**

### **Experimental TREF study and numerical simulation**

Philippe Lodefier\*, Daniel Daoust, Alain M. Jonas and Roger Legras

Unité de Chimie et de Physique des Hauts Polymères,

Université catholique de Louvain, B-1348 Louvain-la-Neuve, Belgium

**SUMMARY:** The fractionation of a statistical copolyester made of poly(ethylene terephthalate- isophthalate) has been performed using Temperature Rising Elution Fractionation (TREF). TREF fractions were analyzed by size exclusion chromatography, thermal analysis, <sup>1</sup>H-nuclear magnetic resonance and small angle X-Ray diffractometry. Results show that the fractions exhibit both interchain and intrachain defect distribution. As the intrachain defect distribution can not be determined by experimental techniques, a computer simulation based on the determination of terephthalic sequences length in a virtual polymeric distribution was performed. The simulated chains were constructed using a stochastic process. The analysis of the results obtained on the distribution of the simulated sequences in the polymer correlates quantitatively well between the new fractionation mechanism proposed for copolyesters and the experimental results.

### **Introduction**

Poly(ethylene terephthalate-isophthalate) (PETI) is a copolymer synthesized from terephthalic acid, isophthalic acid and ethylene glycol by a classical two stages polycondensation. As demonstrated by Berghmans<sup>1)</sup> et al., poly(ethylene isophthalate) (PEI) and poly(ethylene terephthalate) (PET) crystallize in different crystal lattices and cannot cocrystallize. This one explains why increasing the isophthalic content in PET leads to a decrease of copolymer crystallinity and of melting temperature. Increasing the comonomer content coincides with decreasing the average length of regular (crystallizable) sequences in copolymers. However, the copolymer crystallizability is not only dependent on the average comonomer content; as it has been mentioned by various authors, it also depends on structural

parameters such as the number of defects and the distribution of those defects between the chains (interchain distribution) and within the chains (intrachain distribution). Therefore, when dealing with PETI copolymers, in addition to the usual mass distribution of polycondensation polymers we need also to consider the statistical distribution of isophthalic units in PETI. This distribution will govern both the crystallization and the melting behavior of the copolymer.

Experimental information about the statistical interchain distribution of co-monomer can be obtained by Temperature Rising Elution Fractionation (TREF). As already demonstrated for olefinic copolymers<sup>3,4)</sup>, this method allows to separate the sample in different fractions based on differences in co-monomer content between the different chains. Obviously, samples cannot be fractionated by TREF on the basis of their intramolecular distribution of co-monomer. By contrast, the Stepwise Isothermal Segregation Technique (SIST), which is an isothermal crystallization by steps, is well suited to visualize the effects of co-monomer distribution on the melting behavior<sup>2)</sup>; however it is not capable to determine quantitatively the distribution of the lengths of the crystallizable sequences.

The preparative TREF is a fractionation method based on the crystallizability of a polymer in solution. It has been mainly widely applied to the characterization of polyethylene and ethylene/ $\alpha$ -olefin copolymers. Very extensive reviews of TREF applications were published by Wild<sup>3)</sup> and Soares<sup>4)</sup>. The TREF process can be divided into two main steps. During the first step a polymer solution is slowly cooled down. As the temperature is lowered, chains with sufficiently long crystallizable sequences crystallize on an inert support in the fractionation column. The polymer gradually coats the support in successive layers. Layers far off the support are less crystallizable than the closer layers, i.e., they should contain regular sequences of shorter length. The efficiency of the TREF fractionation will depend on the ability of the polymer to segregate into different layers of different crystallizability.

During the second step, fresh solvent is flushed through the column at different temperatures. The polymer layers are then successively eluted, with inner layers collected at higher elution temperatures than outer ones. In a recent paper we have applied for the first time TREF to polycondensation products. It was shown that

TREF elution temperature correlates with diethyleneglycol (DEG) content in the PET chains<sup>5)</sup>.

In the present paper, we couple TREF and SIST experiments complemented with numerical simulations to get information on the inter- and intramolecular distribution of isophthalic units in a PETI copolymer.

This paper will be organized in two parts: the first one centers on the characterization of PETI fractions by different techniques: size exclusion chromatography (SEC), <sup>1</sup>H-Nuclear Magnetic Resonance (<sup>1</sup>H-NMR), small angle X-rays scattering (SAXS) and differential scanning calorimetry (DSC) after SIST crystallization.

In the second part of the paper, we perform a numerical simulation in order to understand the separation process of TREF and to attempt to gain the intramolecular co-monomer distribution.

## **Experimental**

### ***Materials***

The copolymer terephthalic-isophthalic acid was supplied by Imperial Chemical Industries. The copolymer used in this study contains 23% of isophthalic acid and 77% of terephthalic acid (molar ratio).

### ***Fractionation method***

The TREF was carried out in a home made column containing an inert support (iron net). The temperature of the column was controlled using a Julabo F32 thermal controller (30-200 ± 0.01°C). The polymer (5g) was first dissolved in 300 ml of trichlorobenzene (TCB, purchased from ACROS) containing 2% Irganox 1010 to prevent oxidative degradation and then poured into the column at 200°C. After 1 hour the oil bath temperature was programmed to decrease from 200°C to 30°C at a rate of 1.5°C h<sup>-1</sup>. After crystallization of the polymer on the support the temperature of the column was gradually raised in a stepwise manner and flushed at each step with heated TCB. The elution step was stopped when no more polymer was collected. Samples eluted at different temperatures were recovered by precipitation in a large excess of methanol, filtered and vacuum dried.

## Characterization techniques

### NMR

$^1\text{H}$ -NMR Spectra were recorded on a Bruker 500 MHz FT-NMR instrument at room temperature. Polymer samples were dissolved in a mixture of Chloroform-*d* and trifluoroacetic acid (10% v/v). The polymer sample concentration was  $2.5\text{ g l}^{-1}$ . Chemical shifts are quoted in ppm from TMS.

The chemical shift of the isophthalic centered triads have been assigned by Yamadera<sup>6)</sup> and Abis<sup>7)</sup>. The analysis of the spectra was performed using an homemade numerical procedure using the software Igor Pro (Wavemetrics). The spectra were decomposed into the sum of signals from three types of isophthalic centered triads ( III (iso-iso-iso) , TIT (tere-iso-tere) , TII (tere-iso-iso)) with the chemical shifts between the different triads kept constant as well as the relative intensity of the peaks within the same triplet. The attribution of peaks is given in table 1.

table 1:  $^1\text{H}$ -NMR attribution of the isophthalic centered triads.

Triads type	III	IIT	TIT
shift (ppm)	7.652	7.657	7.662
	7.668	7.673	7.678
	7.684	7.688	7.693

The calculation of the isophthalic global content was performed on the basis of other aromatic protons of terephthalic (8.21 ppm) and isophthalic acid (8.81 ppm).

### SEC

Size exclusion chromatography (SEC) analysis was performed with a mixture of hexafluoroisopropanol (HFIP) and chloroform as solvent ( 98/2  $\text{CHCl}_3/\text{HFIP}$ ). The flow rate was 0.8 ml/min. Two Waters HR 5E styragel columns were used in series. The detection was made by a Waters 2486 UV detector at 254nm. A universal calibration curve was established from various polystyrene (PS) standards using the the Mark-Houwink coefficient for PS and PET published by Fox et al<sup>8)</sup>. Samples were dried overnight under vacuum before analysis.

## **SAXS**

For SAXS measurements, samples were compression molded at 280°C in a 200µm aluminium spacer between two Kapton® sheets. The films were crystallized under the press at 0.8°C/min cooling rate.

The SAXS measurements were performed in an evacuated compact Kratky camera equipped with a Braun position sensitive proportional counter. Copper-filtered K $\alpha$  radiation was used from a rotating anode operating at 40kV and 300mA. The data were parasitic- and background-corrected as described elsewhere<sup>9</sup>, then desmeared using a variant of Glatter's algorithm<sup>10</sup>. The long period was calculated from the maximum of the Lorentz-corrected peak; the lamellar thickness was calculated from the correlation function using simplified relationships<sup>11</sup>.

## **DSC (SIST)**

Stepwise Isothermal Segregation Technique (SIST) experiments were carried out in a Perkin-Elmer DSC7 calorimeter. The apparatus was calibrated against indium and tin for temperature and against indium for enthalpy.

The polymer samples were heated in the DSC instrument from 30°C to 280°C. After holding temperature for 5 minutes the samples were rapidly cooled (80°C/min) to 215°C and maintained at that temperature for 1 h. The sample was then successively kept for 1h at each of the following temperatures : 200, 175, 160, 145, 130, 115 °C and finally cooled to 30°C at a rate of 80°C min<sup>-1</sup>. After the crystallization procedure, an usual scanning experiment at 10°C min<sup>-1</sup> was performed to obtain the sample thermogram.

## **Simulation principles**

The aim of the simulation is to construct copolymer chains by a numerical stochastic process and analyze the resulting terephthalic sequence lengths.

Chains of 5 different lengths have been build. A single chain is constituted of  $n_i$  monomers. The number of chains ( $j_i$ ) of a specified length ( $n_i$ ) simulates in a discrete manner a molecular mass distribution for the copolymer. At the beginning of the simulation, the number of isophthalic units in the total number of monomers ( $n_i \times j_i$ ) is fixed equal to the average percentage of isophthalic units in

the "real" copolymer. As it will be shown later, the distribution of isophthalic units within the real copolymer obeys a binomial law. Moreover copolyesters interchange and equilibrium reactions occurs very rapidly in the melt and lead to the randomization of isophthalic distributions within very short times<sup>12,13</sup>. Hence, in the simulation, a random number between 0 and 1 was generated by the computer for each monomer, if the random number is lower than the chosen isophthalic content, this monomer is isophthalic and a numerical value of 1 is attributed to the monomer; otherwise the monomer is terephthalic and a numerical value of 0 is attributed to the monomer. The next monomer is then selected and a new random number is generated. This operation is repeated for each monomer of the simulation.

The distribution of the number of chains of a specified chain length, i.e. the number of monomers, is described in table 2.

table 2: Distribution of the number of chains ( $j_i$ ) as a function of chain length( $n_i$ )

Chain type	Number of segments ( $n_i$ )	Number of chains ( $j_i$ )
1	30	3000
2	100	7000
3	200	10000
4	260	7000
5	500	3000
Total number of segments in the simulation		
$= 6.11 \times 10^6$		

After the generation process, the length of the terephthalate sequences is calculated on the basis of the numerical value of the monomers and of their position in the chain. The chains are then sorted as a function of their Greatest Sequence Length in the Chain (GSLC) which can be defined as the greatest number of successive terephthalate monomers in a chain. The sorted chains are grouped in categories. Each category contains all the chains that have a GSLC between two limit values. For examples, chains having a GSLC between 29 and 26 are grouped in the same category. Each category contains all the information

for the chains of that category: the length ( $n_i$ ), the individual distribution of sequence length and the GSLC of each chain.

## Results and discussion

### *Experimental results*

The mass histogram of the TREF fractions in figure 1 shows the mass percentage of each fractions as a function of the elution temperature. The main part (50%) of the mass distribution is located between 120 and 150 °C. Fractions close to 30°C or 160°C, as it will be shown later, show the greater deviation in term of isophthalic content and are only a small part of the whole polymer. The properties of the 120-150°C fractions will be closer to the average values. We note also that the 30°C fraction may be contaminated by the presence of low molecular mass compounds such as catalyzers, stabilizers and other additives that are soluble in TCB.

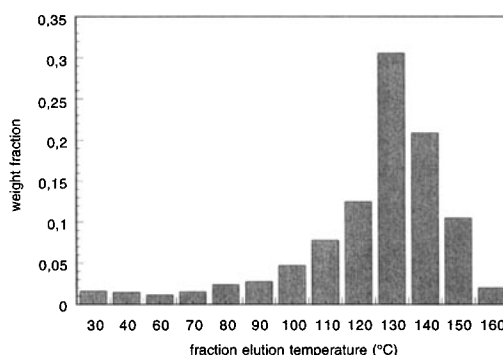


figure 1: mass distribution as a function of the TREF elution temperature

Figure 2 shows the evolution of isophthalic content as a function of elution temperature. Fractions collected at higher temperatures contain less isophthalic moieties than fractions collected at lower temperatures. The observation of a decreasing isophthalic content with increasing elution temperature is consistent with usual TREF results where the concentration of defects decreases with increasing elution temperature and with the results previously reported by Berghmans et al.<sup>1)</sup> for the crystallinity of isophthalic/terephthalic copolymers.

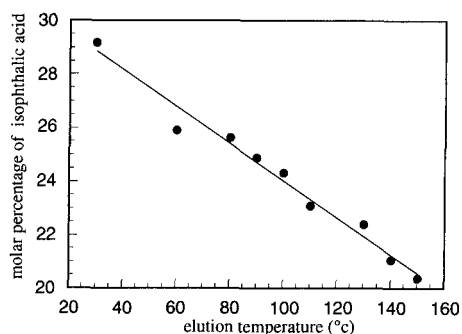


figure 2: Evolution of isophthalic content determined by NMR as a function of TREF elution temperature.

The SEC analysis of the fractions is presented in figure 3. At 30°C of elution temperature we observe a peak of very low molecular mass compounds. This may be attributed to oligomers and additives which are soluble at low temperature in TCB. As the elution temperature increased, the mass distributions are shifting left towards higher molecular mass values. The calculated polydispersity of the fractions (H in figure 3) is still large. All the fractions contain chains of various lengths which confirms that the TREF fractionation mechanism is not based exclusively on a molecular mass separation.

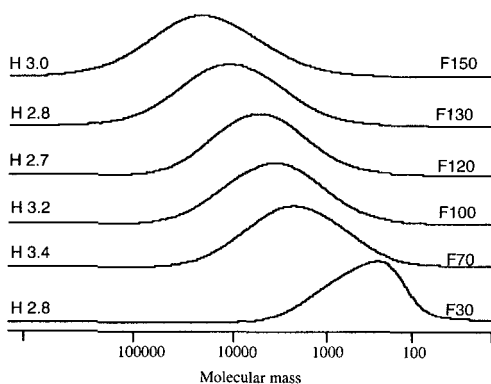


figure 3 : SEC chromatograms of the TREF fractions F30 to F150. Polydispersity indices (H) are reported on the left side of the curve, the elution temperature is reported on the right side.



The statistical distribution of the isophthalic units within each fraction was investigated by  $^1\text{H-NMR}$ . The decomposition of the  $^1\text{H-NMR}$  spectra was performed to obtain the amount of triads centered on isophthalic protons. An example of decomposition is shown in figure 4. The curve (a) reports the original NMR spectra (plain line) and the total fit (dashed line), the curve (b) reports the individual contributions of each proton for the three different types of triads (cfr. table 1 for attribution). It is possible to calculate on the basis of the average isophthalic content of each fraction the theoretical distribution of isophthalic-centered triads. Assuming a binomial distribution for isophthalic units, the distribution of I-centered triads is described by equation (1) and equation (2) .

$$III = P_{iso}^3 \quad \text{equation (1)}$$

$$IIT = P_{iso}^2 P_{tere}$$

$$TIT = P_{iso} P_{tere}^2$$

where:

$P_{iso}$  or  $P_{tere}$  is the molar content of isophthalic or terephthalic units

III = III probability

IIT = IIT probability

TIT= TIT probability

$$III\% = \frac{III}{III + IIT + TIT}$$

$$IIT\% = \frac{IIT}{III + IIT + TIT}$$

$$TIT\% = \frac{TIT}{III + IIT + TIT}$$

equation (2)

III% = III triad percentage

IIT%= IIT triad percentage

TIT%= TIT triad percentage

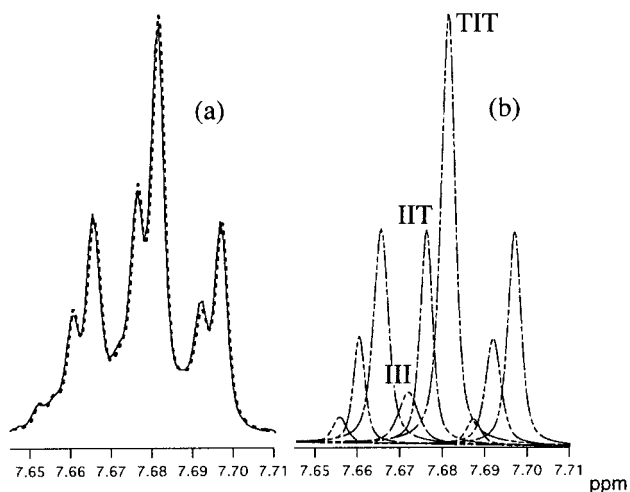


figure 4 :example of NMR deconvolution.

(a) :  $^1\text{H}$ -NMR spectra( plain line) + fit (dashed line); (b): individual peaks for the III, IIT and TIT triads as found by decomposition. The symbol on the peak indicates the center peak of the triad as defined in table 1.

Table 3 provides a comparison between the calculated (equation2) and measured distributions of I-centered triads. The correlation between the theoretical and experimental values is satisfactory given the narrow range of isophthalic content in the fractions. Consequently we may safely conclude that each fraction obeys a binomial statistic. This information will be helpful for performing numerical simulations.

Table 3: Comparaision between the theoretical and experimental values for the content in isophthalic centered triads of each TREF fractions.

Fraction elution temperature (°C)	% III		%IIT		%TIT	
	Theo	Exp.	Theo	Exp.	Theo	Exp.
60	8.9	4.3	24.4	28	66.7	68
80	8.0	3.8	23.4	31	68.6	67
90	7.5	5.7	22.9	26	69.6	68
100	7.1	4.2	22.3	28	70.6	68
110	6.6	4.2	21.8	26	71.6	70
120	6.2	9.1	21.2	27	72.6	62
130	5.8	4.6	20.7	27	73.5	68
140	5.4	8.3	20.1	24	74.5	67
150	5.1	3.4	19.5	25	75.4	72

The SIST crystallization (figure 5) was performed on three fractions, namely F80, F140 and F150, the number referring to the elution temperature of the fraction. The thermograms after SIST show multiple melting peaks, reflecting the presence of species that have been crystallized at different temperatures (that have different crystallizability) and will melt at different temperatures. Only the peak maximum of the final melting peak is shifted to lower temperature when elution temperature decreases. It is important to remember that polypropylene/polyethylene TREF samples subjected to SIST exhibit a different behavior<sup>14</sup>. For such polymers, the melting peaks are much narrower than for the unfractionated polymer and the melting point are increasing as one goes from fractions obtained at lower temperatures to those obtained at higher temperatures.

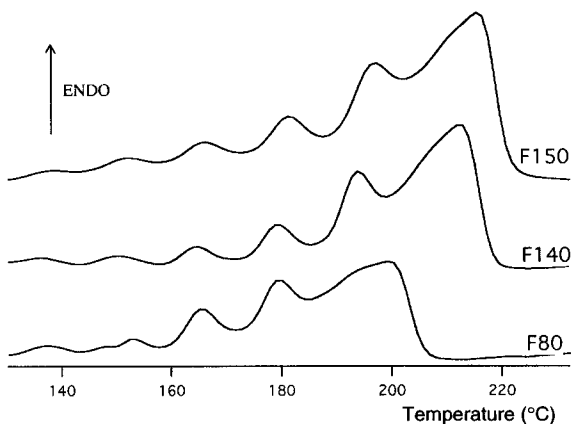


figure 5 :SIST thermograms (10°C/min) of the TREF fractions F80, F140 and F150.

The behavior of our PETI fractions indicates that they still contain a wide distribution of length for the regular terephthalic sequences. Our results are compatible with a process by which chains are sorted as a function of their longest crystallizable sequence. The remaining part of the chain contains still a wide distribution of sequence length. This process can explain the increase of the final melting points together with the presence of multiple peaks for each fraction after SIST.

The SAXS analysis of some TREF fractions allows to evaluate the lamellar thickness ( $l_c$ ) and the long period ( $L$ ) of the samples. The lamellar thickness and long period of the raw sample are reported in table 5 to allow the comparison with the TREF fractions. The long period values range from 119.4 to 129.7Å, while the lamellar thickness lies between 36.1 and 40.6Å. The increase of the long period could be due to the variation of molecular mass between the different fractions as shown by Robelin-Souffaché and Rault <sup>15)</sup>. These authors have also shown that the crystal thickness of PET is molecular weight independent. Therefore, the increase of  $L_c$  with elution temperature may be ascribed to the presence of longer crystallizable sequences in the fractions eluted at higher temperatures, which is compatible with the DSC results. Moreover, we found that the peaks in the SAXS correlation function are very broad, indicating a large distribution of crystal thicknesses. For sample F150, this effect was so predominant that we could not safely obtain a value for the crystal thickness. These results are consistent with the previous DSC/SIST observations.

table 4: Long period ( $L$ ) and lamellar thickness ( $l_c$ )  
of the TREF fractions crystallized at  $-0.8^\circ\text{C}/\text{min}$  from  $280^\circ\text{C}$ .

	$L$ (Å)	$l_c$ (Å)
PETI	125.7	39.2
F80	119.4	37.1
F90	124.4	36.6
F110	124.2	40.0
F140	128.8	40.6
F150	129.7	*

### ***Simulation***

### ***Results and discussion***

We have first checked the stochastic character of the generated distribution. When calculating the triads distribution using probabilistic theories the molecular mass of the chain is assumed to be infinite. The III triads content calculated in the simulation for the chains of different lengths ( $n_i$ ) and for an isophthalic content of 44% can be extrapolated after curve fitting to infinite molecular mass and returns

a value of 0.0398. The theoretical value calculated using equation (1) and equation (2) gives a value of 0.04 for the same isophthalic content and is in good agreement with the value extrapolated from the simulation. Thus we conclude that the isophthalic distribution in the simulated chains obeys also a binomial distribution and reflects well the stochastic character of the real copolymer.

A simulation was performed using a composition of 80% terephthalic acid with the parameters given in table 2. Figure 6 shows the number of T-sequences (i.e., all terephthalic sequences) of a given length for chains sorted by GSLC ( five categories, 29-26, 25-22, 21-18, 17-14, 13-10)

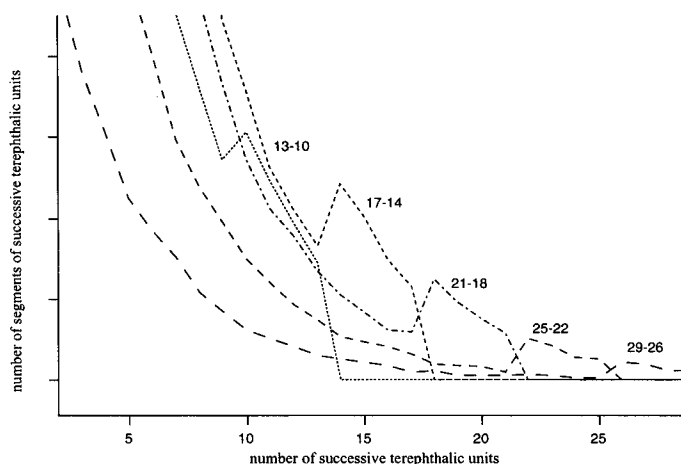


figure 6: number of T-sequences as a function of their length, sorted by GSLC in five categories  
the GSLC of each category is reported in the graph (13-10; 17-14; 21-18; 25-22; 29-26)

Each curve is made off three distinguishable parts as a function of decreasing sequence length: a peak is followed by a depression and then an increase for the probability at lower sequences lengths. The peak is composed of the GSLC sequences which specify each category. Its surface is proportional to the number of chains belonging to the category. The chains carry, in addition to long successive terephthalate sequences, a lot of smaller sequences. The contribution of those smaller T-sequences to the histogram can be visualized on the right side of the peak. This simulation confirms that when sorting the chains on the basis of their GSLC we seize at the same time a lot of smaller T-sequences. As was

mentioned very early by Flory<sup>16)</sup>, the ability to crystallize, at a defined temperature, of a very long successive terephthalate sequence is greater than the one of a shorter sequence. Hence during the TREF fractionation process, the longest crystallizable sequences will crystallize first and will immobilize simultaneously the shorter terephthalate sequences also present in these chains. As the temperature is lowered, chains bearing shorter GSLC will crystallize and so on. The sorting of the chains during the TREF will occur with the GSLC as basis, the role of shorter T-sequences being only marginal. As a consequence, in a given fraction, sequences of very different length will co-exist. This is the reason for the wide distribution of sequences length in our TREF fractions, as evidenced by SIST and SAXS.

The existence of a depression in the histogram distribution arises from the finite chain length of the chains. For the long GSLC categories histograms, the probability of finding another long sequences just below the GSLC is low. The probability to find a lot of smaller successive terephthalate sequences is higher. Note that this would not be the case for infinite chains. Usual probabilistic theories where the chain length is assumed to be infinite do not take this effect into account; for such theories, the probability of finding successive terephthalic sequences is only terephthalic content dependent.

The analysis of the isophthalic content in the different categories is given in table 6.

table 5: determination of the isophthalic content  
in the different categories sorted by GSLC

Category of GSLC	% isophthalic units
29-26	0.127
25-22	0.164
21-18	0.169
17-14	0.204
13-10	0.240
9-6	0.290

When sorting the chains by decreasing GSLC, the isophthalic content in a category is decreasing. This is in good qualitative agreement with the experimental results: lower I-content are found for fractions eluted at larger temperatures (corresponding to larger GSLC). The calculated values for the isophthalic content range between 0.12 and 0.29 when the average isophthalic value of 0.20 is selected for the whole polymer. This results show that in the case of a statistic copolycondensation the deviations from the average values of isophthalic content are large between different chains. The difference in melting points observed by DSC can thus be explained by differences in the length of the crystallizable blocks<sup>17,18</sup>, and also by differences in isophthalic content<sup>16</sup>.

The molecular mass polydispersity inside a TREF fraction can be evaluated by computing the number of chain of each length ( $n_i$ ) as defined in the simulation (cfr. table 2) in a single GSLC category. These data are reported in figure 7 for three different categories.

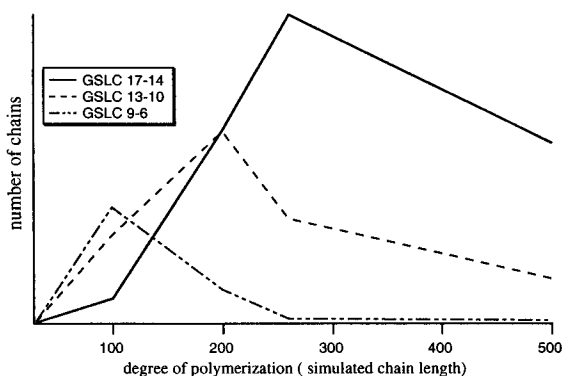


figure 7 : computed number of chains as a function of the simulated chain length for different categories of GSLC.

The position of the peaks on figure 7 is shifted to larger molecular mass for chains of lower GSLC. Again the simulation results corroborates well with the experimental part (SEC study), provided on accepts that TREF separates the chains as a function of GSLC.

## Conclusions

We have shown using different analysis methods that the TREF fractions of a PETI copolymer exhibit two types of heterogeneity:

- the first one is called interchain and refers to differences in isophthalic content, molecular mass, melting temperature and lamellar thickness between the fractions
- the second type of heterogeneity is called intrachain and has been noticed through molecular mass polydispersity, multiple melting temperatures and large distribution of lamellar thickness inside each fraction.

To explain this double behavior, we had to reconsider the TREF separation process with the help of a numerical simulation. We have shown that the separation of chains following their GSLC (greatest sequence length in the chain) shows good correlations between experimental and simulation results. The crystallizability of a chain can be defined, in this case, as the existence within a single chain of a long enough crystallizable sequence. The crystallization of that sequence will immobilize the chain which carries in addition to that long sequence, a lot of smaller crystallizable sequences.

We have also shown the ability of TREF to fractionate copolyesters. The large intrachain distribution of defects in those materials does not produce fractions with very well defined characteristics (narrow molecular weight distribution, single melting temperature,...). As the utility of TREF fractionation is not to be discussed for polyolefins, the question can be raised for copolycondensation products like PETI.

## Acknowledgments

The authors thank Dr. W.M. McDonald (Dupont) for furnishing materials. We would also like to gratefully thanks Pr. J. Devaux (Catholic University of Louvain) for his endless discussions on copolyesters statistical treatments. P. Lodefier is supported by the "Fonds pour la formation à la recherche dans l'industrie et dans l'agriculture" (F.R.I.A ,Belgium).



## References

- <sup>1</sup> H. Berghmans, F. Govaerts, N. Overbergh, *J. of Polym. Sci., Polym. Phys. Ed.*, **17**, 1251 (1979)
- <sup>2</sup> B. Wolf, S. Kenig, J. Klopstock, J. Miltz, *J. Appl. Polym. Sci.*, **62**, 1339 (1996)
- <sup>3</sup> L. Wild, *Adv. Polym. Sci.*, **98**, 1 (1990)
- <sup>4</sup> J.P.B. Soares, A.E. Hamielec, *Polymer*, **36**, 1639(1995)
- <sup>5</sup> P. Lodefier, A. Jonas , R. Legras, *Macromol.*, to be published in 1999
- <sup>6</sup> R. Yamadera , M. Murano, *J. of Polym. Sci.: Part A1: Pol. Chem.*, **5**, 2259 (1967)
- <sup>7</sup> L. Abis, L. Po, S. Spera, G. Bacchilega, O. Occhiello, F. Garbassi, *Makromol. Chem.*, **193**, 1859 (1992)
- <sup>8</sup> B. Fox, M. Moad, G. van Dipen, I. Willing, W. Cook, *Polymer*, **38**, 3035 (1997)
- <sup>9</sup> T.P. Russell , in *Handbook of Synchrotron Radiation*, G. Bbrow and D.E. Monston, Eds., Elsevier, , **3**, 379 (1991)
- <sup>10</sup> O. Glatter, *J. Appl. Cryst.*, **7**, 147 (1974)
- <sup>11</sup> G.R. Strobl, M. Schneider, *J. of Polym. Sci.: Polym. Phys. Ed.* , **18**, 1343 (1980)
- <sup>12</sup> W.S. Ha, Y.K. Chun, S.S. Jang, D.M. Rhee, C.R. Park, *J. Polym. Sci., Part B: Polym. Phys.* , **35**, 309 (1997)
- <sup>13</sup> S.S. Jang, W.S. Ha, W.H. Jo, J.H. Kim, C.R. Park, *J. Polym. Sci., Part B: Polym. Phys.*, **36**, 1637 (1998)
- <sup>14</sup> T. Kamiya , N. Ishikawa, S. Kambe, N. Ikegami, H. Nishibu, T. Hattori, *Soc. Plast. Eng. ANTEC Proceed.*, 871 (1990)
- <sup>15</sup> E. Robelin-Souflaché, J. Rault, *Macromolecules*, **22**, 3581 (1989)
- <sup>16</sup> P.J. Flory, *Trans. Farad. Soc.*, **51**, 848 (1955)
- <sup>17</sup> R.C. Domszy, R. Alamo, C.O. Edwards, L. Mandelkern, *Macromolecules*, **19**, 310 (1986)
- <sup>18</sup> R.C. Domszy, R. Alamo, C.O. Edwards, L. Mandelkern, *J. Polym. Sci., Polym. Phys. Ed.*, **22**, 1727 (1984)